Published in final edited form as:
Insect Mol Biol. 2010 February ; 19(1): 49–60. doi:10.1111/j.1365-2583.2009.00929.x.

Identification and characterization of odorant-binding protein 1 gene from the Asian malaria mosquito, *Anopheles stephensi*

Meryem Senay Sengul[*] and **Zhijian Tu**
Department of Biochemistry, Virginia Polytechnic Institute and State University, Blacksburg, VA, 24061, USA

Abstract

Insect odorant-binding proteins (OBPs) are small, water-soluble molecules that are thought to transport the hydrophobic odorants to their receptors in the chemosensory neurons. Here we report the identification and molecular characterization of *AsteObp1*, an *Obp1* gene in *Anopheles stephensi*, a major malaria vector in Asia. We showed that *AsteObp1* and *Anopheles gambiae Obp1* (*AgamObp1*) are orthologues. These two genes share similar coding sequences and conserved non-coding sequences (CNSs) that may be involved in their regulation. Transcript of *AsteObp1* was observed in larvae and reached a relatively high level in late pupae. Quantitative RT-PCR on female adult chemosensory tissues showed ~900-fold higher expression of *AsteObp1* in antennae than in maxillary palp and proboscis. The amount of *AsteObp1* in female legs was approximately 15-fold lower than that of maxillary palp and proboscis. The level of *AsteObp1* transcript was 7 and 85-fold higher in females than in males in the antennae, and maxillary palp and proboscis, respectively. Moreover, *AsteObp1* level was reduced by approximately 20-fold in maxillary palp and proboscis 24 h after a bloodmeal. Our results indicate that *AsteObp1* likely functions in female olfactory response and it may also be involved in blood-feeding behaviour.

Keywords

antennae; blood-feeding; comparative genomics; olfaction

Introduction

Mosquito behaviours are mediated by both internal and external factors and olfactory cues are undoubtedly the most important external stimuli that affect behaviours such as host-seeking, oviposition, and sugar-feeding (Takken & Knols, 1999). With the availability of the genome assembly of *An. gambiae* and *Ae. aegypti* (Holt *et al*., 2002; Nene *et al*., 2007) and through the advent of behavioural, physiological, and molecular studies (e.g., Takken & Knols, 1999; Takken *et al*., 2001; Meijerink *et al*., 2001; Dekker *et al*., 2002, Justice *et al*., 2003; Xu *et al*., 2003; Hallem *et al*., 2004; Biessmann *et al*., 2005; Zhou *et al*., 2008; Sengul & Tu, 2008), our understanding of the basis for the sense of smell in mosquitoes has been greatly improved in recent years.

In insects, the proteins that are known to be involved in processing of olfactory cues include odorant-binding proteins (OBPs; Vogt & Riddiford, 1981), odorant receptors (ORs; Clyne *et al*., 1999; Vosshall *et al*., 1999), and odorant-degrading enzymes (ODEs; Vogt & Riddiford, 1981; Vogt *et al*., 1999; Ishida & Leal, 2002). Among these, OBPs are believed to bind the

Correspondence: Zhijian Tu, Department of Biochemistry, Virginia Polytechnic Institute and State University, Blacksburg, VA, 24061, USA. Tel: 540-231-8062; Fax: 540-231-9070; jaketu@vt.edu.
[*]Current address: Division of Chemical Ecology, Department of Plant Protection Biology, SLU, Box 102, 230 53 Alnarp, Sweden

odorant molecule and transport it through the aqueous sensillar lymph to the receptors on chemosensory neurons. OBPs are small (15-17 kDa), water-soluble, extracellular proteins present in the sensillum lymph of the sensilla. Most insect OBPs share a hallmark feature of six cysteines, whose relative positions are conserved. A *D. melanogaster* OBP mutant, named *lush*, shows abnormalities in the perception of the aggregation pheromone, 11-cis-vaccenyl acetate (VA) (Xu *et al*., 2005). Moreover, it has been demonstrated that LUSH is required to stimulate the VA-sensitive receptorto elicit a respond to VA (Ha & Smith, 2006). This response is mediated by the pheromone-induced conformational shifts in the LUSH protein (Laughlin *et al*., 2008).

In Diptera, the genomes of the *D. melanogaster*, *An. gambiae*, and *Ae. aegypti* encode 51, 57, and 66 *Obp* genes, respectively (Galindo & Smith, 2001; Hekmat-Scafe *et al*., 2002; Vogt, 2002; Xu *et al*., 2003; Zhou *et al*., 2008). Among OBPs in *An. gambiae*, *AgamObp1* was found at high levels in female antennae, although the expression was observed in headless bodies as well (Biessmann *et al*., 2002; Li *et al*., 2005). Moreover, *AgamObp1* transcript level was reduced after blood-feeding by less than 2-fold in female heads (Justice *et al*., 2003; Biessmann *et al*., 2005), which may indicate a possible role of this gene in blood-feeding behaviour of female mosquitoes.

In this study, we cloned, mapped, and characterized the *Obp1* gene in *An. stephensi* (henceforth referred as *AsteObp1*), an important malaria vector in Asia. Comparisons with *Obp1* gene and protein sequences in other mosquitoes revealed conserved gene structure, potential regulatory sequences, and conserved secondary structure. We also determined the expression profiles of *AsteObp1* using qualitative and quantitative RT-PCR. Our results indicate that *AsteObp1* likely functions in female olfactory response and it may also be involved in blood-feeding behaviour.

Results

Identification and chromosomal mapping of OBP1 in An. stephensi

Obp1 gene (accession number: AY146721; Xu *et al*., 2003) and *Obp17* gene (accession number: AY146723; Xu *et al*., 2003) in *An. gambiae* were previously annotated as two genes that are likely derived through gene duplications since they are found in close proximity to each other on the 2R chromosome, sharing similarity in their flanking sequences as well (Xu *et al*., 2003). A later study also determined different contigs that have identical sequences to predicted OBP1 (Li *et al*., 2005). Currently, the updated Ensembl and Vectorbase annotation shows only a single gene with two possible transcripts in *An. gambiae*: Q8I8TO_ANOGA (AY146721) and OBP17 (AY146723). Q8I8TO_ANOGA codes for the *Agam*OBP1 peptide (AF437884; Biessmann *et al*., 2002). We used the gene sequence of *AgamObp1* to construct an *Obp1* gene probe to screen a bacterial artificial chromosome (BAC) library derived from *An. stephensi* genomic DNA. Three positive clones were identified from a total of 9216 clones screened, which represents ~ 5-fold coverage of the genome, assuming that the genome size of *An. stephensi* is approximately 240 Mbp (Rai and Black, 1999). One positive BAC clone was sequenced, which produced 2 contigs. A single *An. stephensi Obp1* gene (*AsteObp1*, FJ410801) was identified in the 98.5 kb assembled contig sequence (GQ250942).

Furthermore, we mapped *AsteObp1 gene* to the region corresponding to 17A of the chromosomal arm 2R of the ovarian chromosomes of *An. stephensi* by fluorescent *in situ* hybridization analysis (Fig. 1). This region is homologous to *An. gambiae* 14E of chromosomal arm 2R, the region in which *AgamObp1* gene resides (http://www. ensembl.org/Anopheles_gambiae/index.html; Sharakhova *et al*., 2006). Our chromosomal mapping and sequence analysis (discussed below) indicate that the *AsteObp1*

gene is located at a single locus in the *An. stephensi* genome and *AsteObp1* and *AgamObp1* are probably orthologues.

Comparison of the Obp1 *genomic regions in* An. gambiae *and* An. stephensi

Fig. 2A shows the VISTA display of the sequence alignment between *An. gambiae* and *An. stephensi* in the genomic regions including the *Obp1* gene and nearby sequences. The coding sequences of the *Obp1* genes as well as the order of neighboring genes are conserved between the two species. For example, a homologue of the *An. gambiae* G-protein coupled odorant receptor *GPROr66* gene, which is next to the *AgamObp1* gene, is also identified approximately 10 kb downstream of the *AsteObp1*. We named this gene as *AsteGPROr66* (FJ410800).

Pairwise alignment revealed high level of conservation in the coding regions of *Obp1* gene, ranging between 77% to 94% identity at the nucleotide level. Additionally, there are a few conserved non-coding sequences (CNSs) at the 5′ and 3′ flanking regions as well as in an intron (Fig. 2A, pink peaks). These regions exhibited 71% to 87% identity between the two species. In order to determine whether these regions contain any transcription factor binding sites (TFBSs), we used ConSite prediction tool (Sandelin *et al*., 2004) and found significant hits for C2H2-type zinc finger (*Broad-complex* isoforms 1 and 4), a nuclear receptor factor (*RXR-VDR*) and HMG (*Sox*) binding sites ~1.1 kb upstream of the *Obp1* gene. These sites are conserved between *An. gambiae* and *An. stephensi* (Fig. 2B). Interestingly, the conserved segment (the pink peak, Fig. 2A) in the second intron of *Obp1* also contained TFBSs for an ecdysone-induced transcription factor *E74A* and another nuclear receptor factor (*CFI-USP*) (data not shown). Other highly conserved motifs have also been observed in the pairwise alignment that did not show any significant hits for a known transcription factor in the database.

Experimental characterization of AsteObp1 *gene structure*

The *AgamObp1* gene model served as a good reference for the annotation of the *AsteObp1* coding sequences. The alignment shown in Fig. 2A suggests a good conservation in the coding sequences of *AsteObp1* and *AgamObp1* genes. The observed conservation between *AgamObp1* and *AsteObp1* genes also helped the identification of a potential TATA-box and the transcription start site. A TCAGT sequence (Fig. 3A, boldface and italicized), which is identical to the arthropod initiator consensus (Cherbas & Cherbas, 1993), is observed 69 nucleotides upstream of the translation initiation codon, ATG. A consensus for TATA-box is located 101 bp upstream of the ATG as well (Fig. 3A; boldface and boxed).

The 3′ end of the *AsteObp1* transcript was determined by 3′ RACE, which produced a cDNA product with an expected poly(dA) tail, a 422 bp untranslated region (UTR) and a removed intron. Reverse transcription polymerase chain reaction (RT-PCR) was also performed using primers spanning the first predicted intron (Fig. 3A). Comparing sequences of the RT-PCR and RACE products and the BAC clone confirmed the existence the first and second introns of 121 bp and 461 bp in length, respectively. Overall, we characterized the entire open reading frame (ORF) of *AsteObp1* interrupted by two introns as shown in Fig. 3A. The coding region is 432 bp long encoding a 144 amino acid peptide. The overall gene structure of *AsteObp1* is highly similar to that of *AgamObp1* (Fig. 3B), which is annotated in GenBank (AY146721; Xu *et al*., 2003).

Expression profile of AsteObp1

The expression profile of *AsteObp1* was initially examined by non-quantitative RT-PCR. We found a higher level of *AsteObp1* expression in late pupae compared to larvae or early pupae (Fig. 4A). Either weak expression or nearly no expression was observed in the first

instar larvae, late larvae, and early pupae. We also performed RT-PCR using different olfactory and gustatory tissues from 1-day-old and 5 to 6-days-old adults of both sexes as well as females 24 h after a bloodmeal. Broad distribution of *AsteObp1* gene expression in most of the chemosensory tissues of mosquitoes was observed (Fig. 4B, 4C). *AsteObp1* was expressed in mosquito head tissues such as antennae, maxillary palp and proboscis, and mosquito body parts such as legs and wings. *AsteObp1* expression appeared to be reduced in maxillary palp and proboscis in females after a bloodmeal (Fig. 4C). Either very weak or no expression was observed in body samples devoid of head and appendages (not shown).

Furthermore, quantitative real-time PCR was performed to compare the *AsteObp1* mRNA levels in the antennae, maxillary palp and proboscis, and legs from adult females. We observed a significantly higher (~900-fold) expression in female antennae compared to that of the maxillary palp and proboscis (Fig. 5; Table 1). Very low amount of *AsteObp1* was observed in female legs, approximately 15-fold lower than that of in maxillary palp and proboscis. These results clearly show that *AsteObp1* is much more abundantly expressed in the primary olfactory organ, the antennae, of the *An. stephensi* mosquitoes compared to the other chemosensory tissues. Although the expression level in maxillary palp and proboscis was low, the level was significant and likely biologically relevant.

We also determined expression levels of *AsteObp1* in different tissues between males, females and blood-fed females. We observed a significantly higher expression of *AsteObp1* in the female antennae (~7-fold) and maxillary palp and proboscis (~80-fold) than those in males (Fig. 5B-D). The *AsteObp1* expression in legs was not significantly different between male and females. However, the expression in legs was increased by > 2-fold in blood-fed females. Given the low level of transcripts in the legs, it is unclear whether the difference before and after blood-feeding is biologically relevant. Bloodmeal did not affect the mRNA level of *AsteObp1* in the antennae of female mosquitoes. However, we observed a ~20-fold reduction of *AsteObp1* gene expression in maxillary palp and proboscis of blood-fed females compared to that of females before a bloodmeal.

Conservation of OBP1 protein structure among divergent mosquito species

The deduced amino acid sequences of OBP1 from *An. gambiae*, *An. stephensi*, *Ae. aegypti* and *C. p. quinquefasciatus* were aligned in Fig. 6. Mosquito OBP1 proteins show 76% to 86% amino acid identity, as well as six cysteines whose positions are absolutely conserved. The predicted secondary structure of *AsteOBP1* includes six α-helices (Fig. 6; solid bars above the peptide sequence), consistent with the predicted structures from *Agam*OBP1 and other insect OBPs (Leal *et al*., 1999;Sandler *et al*., 2000;Lartigue *et al*., 2004;Kruse *et al*., 2003;Mohanty *et al*., 2004;Wogulis *et al*., 2006). The N-terminal signal peptide sequence (Fig. 6, underlined) of mosquito OBP1 is less conserved than the rest of the protein.

Selection pressure acting on mosquito Obp1 genes

Pairwise comparisons of mosquito *Obp1* sequences were used to determine the rates of synonymous (d_S) and nonsynonymous (d_N) codon substitutions and the ratio of d_N/d_S was calculated to provide an estimate of the selection pressure on *Obp1* genes in *An. gambiae and An. stephensi*. OBP1 orthologues from divergent mosquito species such as *Ae. aegypti* and *C. p. quinquefasciatus* were not included in the d_N/d_S ratio calculations, because the d_S values were saturated and were not reliable. The coding regions of *Obp1* were included in the analysis except the 5′ exon regions, which encode the signal peptides that are highly divergent among OBPs. The d_N value between *AsteObp1* and *AgamObp1* is 0.022 and the d_S is 0.596. The d_N/d_S ratio is far less than 1, suggesting that *Obp1* is evolving under strong purifying selection for a possibly important function in mosquitoes.

Discussion

In this study, we report identification and characterization of *Obp1* gene from the Asian malaria mosquito *An. stephensi*. We named it *Obp1* gene in *An. stephensi* (*AsteObp1*) because it shows sequence identity and conservation of gene structures with the *An. gambiae Obp1* (*AgamObp1*). Qualitative and quantitative RT-PCR analysis of *AsteObp1* reported here showed predominant expression in the antennae and a strong female-bias. This is consistent with strong expression of *AgamObp1* in female head (Biessmann *et al*., 2005) and supports that *Obp1* may play an important role in adult female antennae, the primary olfactory tissue. Female-biased expression of *AsteObp1* in olfactory organs, such as antennae and maxillary palp and proboscis, may result from a larger number of olfactory sensilla in females than in males (McIver, 1982).

Our analysis of *AsteObp1* expression in larval and pupal stages and quantitative RT-PCR analysis of *AsteObp1* in dissected adult olfactory organs offer several new insights. First, we detected relatively strong expression of *AsteObp1* in late pupae, which either suggests a possible chemosensory role of this gene in pupae or a simple correlation with the onset of development of chemosensory tissues during pupation. Further study is needed to differentiate the above two possibilities. Second, *AsteObp1* transcripts were also detected, albeit at low levels, in gustatory organs, such as legs and wings. It is possible that *AsteObp1* may have a gustatory role. Alternatively, these gustatory tissues might have olfactory capabilities that are yet to be understood in mosquitoes.

Third, although we did not observe significant difference in either the antennae or the leg between non-bloodfed females and females 24 h after blood-feeding, we detected ~ 20-fold reduction of *AsteObp1* transcript level in female maxillary palp and proboscis. This is very interesting as it indicates a possible involvement of *AsteObp1* in blood-feeding behavior. The ORNs of maxillary palpal sensilla in mosquitoes are important in olfaction including detection of CO_2 and 1-octen-3-ol for host localization (Gillies, 1980; Grant *et al*., 1995; Grant & O'Connell, 1996; Dekker *et al*., 2001; Syed & Leal, 2007; Lu *et al*., 2007). The reduction of *AsteObp1* (this paper) and *AsteObp7* transcripts (Sengul & Tu, 2008) in pooled maxillary palp and proboscis after blood-feeding may reflect the decreased need for host-seeking or blood-feeding. It will be interesting to see if such reduction is also observed in *Obp1* homologues of other mosquito species.

Comparative analysis suggests that *Obp1* orthologues underwent little structural changes in mosquitoes. In fact, we determined a strong purifying selection ($d_N/d_S < 1$) among anopheline *Obp1* genes, which is consistent with its proposed functional importance. A better understanding of the functional role of OBPs in olfaction may come from the structural studies of different OBPs in various insect species. In mosquitoes, the crystal structure of OBP1 in *An. gambiae* has been determined (Wogulis *et al*., 2006), representing the only known OBP structure from mosquitoes. This protein is crystallized as a dimer with a unique binding pocket, consisting of a single tunnel running through both subunits. It has been found that *Agam*OBP1 undergoes a pH dependent conformational change, which was initially proposed for the ligand (i.e. bombykol) binding and releasing mechanism for PBP in *B. mori* (*Bmor*PBP) (Horst *et al*., 2001). The alignment of *Aste*OBP1 with *Agam*OBP1 and other mosquito orthologues showed a high level of conservation in the overall protein structure (Fig. 6). The availability of the primary and secondary structure of *Aste*OBP1 will help future modeling studies that compare and contrast the two anopheline OBP1 proteins.

Understanding the regulatory elements that play a role in *Obp1* expression may provide insights into the function of this gene in mosquito olfaction. For this purpose, a comparative approach was used to uncover possible regulatory elements of *Obp1* gene in *An. gambiae*

and *An. stephensi* by determining the conservation in the non-coding regions. Previously, by using a similar approach, we have determined conserved motifs in the 5′ upstream sequences of *Obp7* gene in the three anopheline mosquitoes, including *An. gambiae*, *An. stephensi* and *An. quadriannulatus* (Sengul & Tu, 2008). Although we were unable to experimentally verify the transcription start site of *AsteObp1*, predictions based on the *AgamObp1* gene model points to a conserved transcription start site and upstream TATA box (Fig. 3A). In the 5′ upstream regions of *Obp1* genes, we observed conserved binding sites for *Broad-complex* isoforms and *RXR-VDR* transcription factors both in *An. gambiae* and *An. stephensi*. However, much of the conservation in other regions did not give any hits for a known transcription factor. It is possible that these are novel binding sites that may likely play a role in *Obp* gene regulation in mosquitoes, which need to be experimentally tested. We have also identified a possible odorant receptor gene orthologue of the *An. gambiae GPROr66* gene, approximately 10 kb apart from the *AsteObp1* gene (Fig. 2A). It would be interesting to determine whether the close chromosomal localization of *Obp1* and *Or66* genes in both species has any effect on the regulation of these genes.

Experimental procedures

Mosquitoes and dissections

Anopheles stephensi Indian strain were reared at 27°C with 75% relative humidity. Conditions for dissection and tissue collection were previously described (Sengul & Tu, 2008).

Generation of digoxigenin-labelled, single-stranded DNA (ssDNA) probes and Bacterial Artificial Chromosome (BAC) library screening

An amino acid alignment of *Agam*OS-E (EAA01090; Vogt, 2002), *Agam*OS-F (EAA09615; Vogt, 2002), *Agam*OBP1 (AF4377884; Biessmann *et al*., 2002), *D. melanogaster* OS-F (U02542; McKenna *et al*., 1994), and OS-E (U02543; McKenna *et al*., 1994) has been performed using Clustal X (1.8) (Thompson *et al*., 1997). This alignment was used to design the following degenerate primers; OBP1F1: 5′-TGYTAYATGAAYTGYYTNTTYCA corresponding to the motif CYMVCLFH and OBP1R1: 5′-CARCAYTTRTGNARCCARAANGC corresponding to the motif AFWLHKCW. The genomic DNAs were isolated from *An. stephensi* mosquitoes using DNAzol Genomic DNA Isolation Reagent (Molecular Research Center, Inc., Cincinnati, OH, USA). Degenerate primers (mentioned above) were used to amplify a 186 bp sequence in the second exon region of the *AsteObp1* gene. The PCR product was cloned using pGEM-T-Easy vector systems (Promega, Madison, WI, USA) and confirmed by sequencing (Virginia Bioinformatics Institute, Blacksburg, VA, USA). The plasmid that contains *Obp1* gene sequence was used as a template in an asymmetric PCR using the primer, OBP1probe: 5′-GTTTGTTTCACGAGGCCAAG, and DIG-dUTP labelling mixture (Roche Diagnostics, Indianapolis, IN, USA) to generate ssDNA probe. The DIG-labelled ssDNA probe was used to screen the BAC library of *An. stephensi* under moderate conditions. The average insert size of the *An. stephensi* BAC library is 125 kb and the library represents ~10x coverage of the genome. Hybridization was carried out at 55°C overnight. Two set of washes were performed at 55°C with 2X and 0.5X SSC (Saline Sodium Citrate). Details about the construction and screening of the *An. stephensi* BAC library were previously described (Sengul & Tu, 2008).

BAC DNA sequencing

The positions of the positive clones were determined using the 384-well plate overlay. Single colony preps were made by dipping a sterile inoculating loop into stab (BACs are supplied as stabs in agar) and drawing parallel lines on the LB/chloramphenicol (12.5μg/ml)

plates followed by incubation overnight at 37°C. One positive BAC clone per each screening was selected for BAC DNA isolation that was used to check for the coverage of clones by PCR before sequencing. Sequencing was done at TIGR (The Institute for Genomic Research, Rockville, MD) using Sanger chemistry and the shotgun approach.

Identification of *AsteObp1* and its possible mosquito orthologues

Contigs obtained from *An. stephensi* BAC sequencing were compared to *AgamObp1* using BLAST (Altschul *et al*., 1990). Sequences that had significant match to *AgamObp1* and nearby coding sequences were further analyzed using BLAST and VISTA alignment (http://genome.lbl.gov/vista/index.shtml). The orthologues of OBP1 were obtained from the NCBI database and they include *Aaeg*OBP1 from *Ae. aegypti* (AY189223; Ishida *et al*., 2004), and *Cqui*OBP1 from *C. p. quinquesfasciatus* (AF468212; Ishida *et al*., 2002).

Fluorescent in situ hybridization (FISH) analysis of *AsteObp1*

MapOBP1L: 5′-GCTCGTGTTTGCTTCAGTTG and MapOBP1R: 5′-ACC CACACCGATTAAAGTGC primer pair was used to amplify a 1054 bp genomic sequence of the *AsteObp1* gene, which was confirmed by sequencing (Virginia Bioinformatics Institute). Gel purified PCR product was used to make probe labeling with Cy5-AP3-dUTP (GE Healthcare, Little Chalfont, Buckinghamshire, UK) using Random Primers DNA Labeling System (Invitrogen, Carlsbad, CA, USA). Fluorescently labelled *Obp1* gene probes was used for *in situ* hybridization on the polytene chromosomes of *An. stephensi* females prepared from ovarian nurse cells. Chromosome preparation and hybridization were performed as previously described (Sharakhova *et al*., 2006).

Expression analysis of *AsteObp1* by RT-PCR

Total RNA was isolated from various *An. stephensi* developmental stages and manually dissected 1-day-old and 5-6 days old male and female adult tissues using Trizol reagent (Invitrogen, Carlsbad, CA, USA). Following DNase treatment (Ambion, Inc., Austin, TX, USA), samples were reverse transcribed using Superscript II reverse transcriptase (Invitrogen) at 42°C for 1.5 hr followed by heat inactivation at 70°C for 15 minutes. All cDNA synthesis reactions were carried out in the absence of reverse transcriptase (−RT) in parallel for each sample. RT-PCR amplification of cDNAs were carried out using gene specific primers, RTOBP1L: 5′-GTTTGTGTCGGGTTGATGTG and RTOBP1R: 5′-TTGTCGCAAAGATTTTCACC, that span the first intron sequence of *AsteObp1* gene to control for any genomic DNA contamination. Accordingly, PCR products with an expected size of 356 bp from cDNA amplification can be differentiated from genomic DNA amplification of a 477 bp product. We used *AsteRps4* (EU883624; Sengul & Tu, 2008) as an internal control in the RT-PCR reactions to determine the integrity of cDNA templates. RT-PCR primer pair Rps4L: 5′-CACGAGGATGGATGTTGGAC and Rps4R: 5′-ATCAGGCGGAAGTATTCACC amplified a cDNA product of about 262 bp in length. The optimal annealing temperature for the RT-PCR was 60°C for both *AsteObp1* and *AsteRps4* genes. Both reactions were run for a total of 35 cycles and are not quantitative. PCR products were analysed by 2% agarose-gel electrophoresis.

Quantitative real-time PCR

For quantitative real-time PCR, total RNA from selected tissues was isolated from adult 6-day-old male, 5-day-old female and 6-day-old blood-fed females to perform cDNA synthesis as mentioned above. Our analyses included at least three biological replicates for all samples, each from independent collections. The quantitative real-time PCR was performed using the TaqMan probe-based chemistry with an ABI Prism 7300 Sequence Detection System (SDS; Applied Biosystems, Foster City, CA, USA). For each 25 μl PCR

reaction, 2 μl of cDNA was used with 9.25 μl nuclease-free water, 12.5 μl 2 X TaqMan Universal PCR Master Mix (Applied Biosystems), and 1.25 μl 20 X assay mix designed by ABI. The thermocycler programme consisted of 50°C for 2 min, 95°C for 10 min, 40 cycles of 95°C for 15 sec and 60°C for 1 min. As the relative mRNA amount of *AsteObp1* was being determined, parallel TaqMan assays were also carried out for the control gene, *AsteRps4*. The assay mixture for *AsteObp1* and *AsteRps4*, consisted of 5′FAM (5′-carboxyfluorescein), nonfluorescent quencher (NFQ) labelled probes and the primer pairs as follows:

- *AsteObp1*primerF: 5′-AACCGCTGCACGATATTTGC-3′
- *AsteObp1*primerR: 5′-GGATCTCTTCGTCGCTGAACTTTT-3′
- *AsteObp1*probe: 5′FAM-ATCGCTTCCTCAGTAACAC-NFQ
- *AsteRps4*primerF: 5′-TTCGCACCGATCCGAACTAC-3′
- *AsteRps4*primerR: 5′-GAAGTATTCACCGGTCTTGTGGAT-3′
- *AsteRps4*probe: 5′FAM-TTGATCACATCCATGAAACC-NFQ

All TaqMan PCR data were analyzed using SDS Software based on the comparative method ($\Delta\Delta C_T$) (Livak & Schmittgen, 2001) as previously described (Sengul & Tu, 2008). We used ΔC_Tvalues for statistical analysis of real-time PCR data. One-way ANOVA with Tukey's post test was performed using GraphPad Prism version 3.00 for Windows (GraphPad Software, San Diego, CA, USA). Significance in comparisons was assumed if $P < 0.05$ was obtained in the appropriate test.

Rapid Amplification of cDNA Ends (RACE)

3′ RACE were performed using the BD Smart RACE cDNA amplification kit (BD Biosciences Clontech, Palo Alto, CA, USA) according to the manufacturer's instructions. After the initial cDNA synthesis, PCR was performed using the adapter primer and the gene specific primer (3′RACE: 5′-GGCAAACGATGCCTCTATCC). The PCR products were cloned into pGEM-T-Easy vector (Promega, Madison, WI, USA) and confirmed by sequencing (Virginia Bioinformatics Institute).

Sequence analyses of OBP1

The gene structure of *AsteObp1* was confirmed by RT-PCR and RACE. The peptide alignment of OBP1 orthologues was generated by using CLUSTAL X (1.8) (Thompson *et al*., 1997). The following parameters were used for the alignment: pairwise gap penalty (open=35, extension=0.75), multiple gap penalty (open=15, extension=0.3). N-terminal signal peptide sequences of OBP1 were predicted by the SIGNALP V 3.0 programme (Bendtsen *et al*., 2004; http://www.cbs.dtu.dk/services/SignalP/). Putative α-helical regions were predicted using JPRED (Cuff & Barton, 1999; http://www.compbio.dundee.ac.uk/~www-jpred/). The results of Jpred were confirmed with Swiss-Model, a web based homology modeling program (http://swissmodel.expasy.org/).

Sequence comparison and transcription factor binding site (TFBS) predictions

The genome comparisons to identify conservation in coding and non-coding regions of OBP1 from *An. stephensi* and *An. gambiae* were established by using MLAGAN (Multi-LAGAN; Brudno *et al*., 2003; http://genome.lbl.gov/vista/lagan/submit.shtml). The cut-off for sequence conservation was 75% over 100 bp. The *An. gambiae* genome annotation (Holt *et al*., 2002) was used to determine the coding regions in the alignment. The alignment was visualized by VISTA (Mayor *et al*., 2000), which gave a VISTA plot output calculating the percent identity over the window at each base pair. The x-axis showed the relative position

of the *An. gambiae* genomic DNA, and the y-axis shows the % identity between *An. stephensi* and *An. gambiae* sequences. ConSite program (Sandelin *et al*., 2004; http://asp.ii.uib.no:8090/cgi-bin/CONSITE/consite/) is used to predict potential transcription factor binding sites for the 5′ upstream sequences of *Obp1*, up to 1 kb region from the translation start site, of the aligned sequences between *An. gambiae* and *An. stephensi*. The cut-off for sequence conservation was 74%, and transcription factor score threshold was set to 80%.

d_N and d_S calculations

Synonymous and nonsynonymous mutation rates were analyzed by the method of Nei & Gojobori (1986). The SNAP program (Synonymous/Nonsynonymous analysis program; http://www.hiv.lanl.gov/content/sequence/SNAP/SNAP.html; Korber, 2000) was used to calculate d_N, d_S and to determine d_N/d_S ratios for mosquito OBP1 orthologues.

Supplementary Material

Refer to Web version on PubMed Central for supplementary material.

Acknowledgments

We thank Dr Maria V. Sharakhova for help with *in situ* hybridizations; Thomas R. Saunders for rearing *An. stephensi* mosquitoes. We also thank three anonymous reviewers for their constructive comments. This work was supported by National Institutes of Health Grant AI063252.

Nomenclature

AsteObp1	*Anopheles stephensi* odorant-binding protein 1 gene
***Aste*OBP1**	*Anopheles stephensi* odorant-binding protein 1 protein
AgamObp1	*Anopheles gambiae* odorant-binding protein 1 gene
***Agam*OBP1**	*Anopheles gambiae* odorant-binding protein 1 protein

References

Altschul SF, Gish W, Miller W, Myers EW, Lipman DJ. Basic local alignment search tool. J Mol Biol. 1990; 215:403–410. [PubMed: 2231712]

Bendtsen JD, Nielsen H, von Heijne G, Brunak S. Improved prediction of signal peptides: SignalP 3.0. J Mol Biol. 2004; 340:783–795. [PubMed: 15223320]

Biessmann H, Walter MF, Dimitratos S, Woods D. Isolation of cDNA clones encoding putative odourant binding proteins from the antennae of the malaria-transmitting mosquito, *Anopheles gambiae*. Insect Mol Biol. 2002; 11:123–132. [PubMed: 11966877]

Biessmann H, Nguyen QK, Le D, Walter MF. Microarray-based survey of a subset of putative olfactory genes in the mosquito *Anopheles gambiae*. Insect Mol Biol. 2005; 14:575–589. [PubMed: 16313558]

Brudno M, Do CB, Cooper GM, Kim MF, Davydov E, NISC Comparative Sequencing Program. Green ED, Sidow A, Batzoglou S. LAGAN and Multi-LAGAN: efficient tools for large-scale multiple alignment of genomic DNA. Genome Res. 2003; 13:721–731. [PubMed: 12654723]

Cherbas L, Cherbas P. The arthropod initiator: the capsite consensus plays an important role in transcription. Insect Biochem Mol Biol. 1993; 23:81–90. [PubMed: 8485519]

Clyne PJ, Warr CG, Freeman MR, Lessing D, Kim J, Carlson JR. A novel family of divergent seven-transmembrane proteins: candidate odorant receptors in *Drosophila*. Neuron. 1999; 22:327–338. [PubMed: 10069338]

Cuff JA, Barton GJ. Evaluation and improvement of multiple sequence methods for protein secondary structure prediction. Proteins. 1999; 34:508–519. [PubMed: 10081963]

Dekker T, Takken W, Carde RT. Structure of host odour plumes influences catch of Anopheles gambiae s.s. and Aedes aegypti in a dual-choice olfactometer. Physiol Entomol. 2001; 26:124–134.

Dekker T, Steib B, Carde RT, Geier M. L-lactic acid: a human-signifying host cue for the anthropophilic mosquito *Anopheles gambiae*. Med Vet Entomol. 2002; 16:91–98. [PubMed: 11963986]

Galindo K, Smith DP. A large family of divergent *Drosophila* odorant-binding proteins expressed in gustatory and olfactory sensilla. Genetics. 2001; 159:1059–1072. [PubMed: 11729153]

Gillies MT. The role of carbon dioxide in host-feeding my mosquitoes (Diptera: Culicidae). Bull Entomol Res. 1980; 70:525–532.

Grant AJ, Wigton BE, Aghajanian JG, O'Connell RJ. Electrophysiological responses of receptor neurons in mosquito maxillary palp sensilla to carbon dioxide. J Comp Physiol [A]. 1995; 177:389–396.

Grant AJ, O'Connell RJ. Electrophysiological responses from receptor neurons in mosquito maxillary palp sensilla. Ciba Found Symp. 1996; 200:233–248. [PubMed: 8894301]

Ha TS, Smith DP. A pheromone receptor mediates 11-*cis*-Vaccenyl acetate-induced responses in *Drosophila*. J Neurosci. 2006; 26:8727–8733. [PubMed: 16928861]

Hallem EA, Nicole Fox A, Zwiebel LJ, Carlson JR. Olfaction: mosquito receptor for human-sweat odorant. Nature. 2004; 427:212–213. [PubMed: 14724626]

Hekmat-Scafe DS, Scafe CR, McKinney AJ, Tanouye MA. Genome-wide analysis of the odorant-binding protein gene family in *Drosophila melanogaster*. Genome Res. 2002; 12:1357–1369. [PubMed: 12213773]

Holt RA, Subramanian GM, Halpern A, Sutton GG, Charlab R, Nusskern DR, et al. The genome sequence of the malaria mosquito *Anopheles gambiae*. Science. 2002; 298:129–149. [PubMed: 12364791]

Horst R, Damberger F, Luginbuhl P, Guntert P, Peng G, Nikonova L, Leal WS, Wuthrich K. NMR structure reveals intramolecular regulation mechanism for pheromone binding and release. Proc Natl Acad Sci USA. 2001; 98:14374–14379. [PubMed: 11724947]

Ishida Y, Cornel AJ, Leal WS. Identification and cloning of a female antenna-specific odorant-binding protein in the mosquito *Culex quinquefasciatus*. J Chem Ecology. 2002; 28:867–871.

Ishida Y, Leal WS. Cloning of putative odorant-degrading enzyme and integumental esterase cDNAs from the wild silkmoth, *Antheraea polyphemus*. Insect Mol Biol. 2002; 32:1775–1780.

Ishida Y, Chen AM, Tsuruda JM, Cornel AJ, Debboun M, Leal WS. Intriguing olfactory proteins from the yellow fever mosquito, *Aedes aegypti*. Naturwissenschaften. 2004; 91:426–431. [PubMed: 15338030]

Justice RW, Dimitratos S, Walter MF, Woods DF, Biessmann H. Sexual dimorphic expression of putative antennal carrier protein genes in the malaria vector *Anopheles gambiae*. Insect Mol Biol. 2003; 12:581–594. [PubMed: 14986919]

Korber, B. Computational Analysis of HIV Molecular Sequences. In: Rodrigo, Allen G.; Learn, Gerald H., editors. HIV Signature and Sequence Variation Analysis. Kluwer Academic Publishers; Dordrecht, Netherlands: 2000. p. 55-72.Chapter 4

Kruse SW, Zhao R, Smith DP, Jones DNM. Structure of a specific alcohol-binding site defined by the odorant binding protein LUSH from *Drosophila melanogaster*. Nat Struct Biol. 2003; 10:694–700. [PubMed: 12881720]

Lartigue A, Gruez A, Briand L, Blon F, Bezirard V, Walsh M, Pernollet JC, Tegoni M, Cambillau C. Sulfure single-wavelength anomalous diffraction crystal of a pheromone-binding protein from the honeybee *Apis mellifera L*. J Biol Chem. 2004; 279:4459–4464. [PubMed: 14594955]

Laughlin JD, Ha TS, Jones DN, Smith DP. Activation of pheromone-sensitive neurons is mediated by conformational activation of pheromone-binding protein. Cell. 2008; 133:1255–1265. [PubMed: 18585358]

Leal WS, Nikonova L, Peng G. Disulfide structure of the pheromone binding protein from the silkworm moth, *Bombyx mori*. FEBS Lett. 1999; 464:85–90. [PubMed: 10611489]

Li ZX, Pickett JA, Field LM, Zhou JJ. Identification and expression of odorant-binding proteins of the malaria-carrying mosquitoes *Anopheles gambiae* and *Anopheles arabiensis*. Arch Insect Biochem Physiol. 2005; 58:175–189. [PubMed: 15717318]

Livak KJ, Schmittgen TD. Analysis of relative gene expression data using real-time quantitative PCR and the $2^{-\Delta\Delta CT}$method. Methods. 2001; 25:402–408. [PubMed: 11846609]

Lu T, Qiu YT, Wang G, Kwon JY, Rutzler M, Kwon HW, Pitts RJ, van Loon JJ, Takken W, Carlson JR, Zwiebel LJ. Odor coding in the maxillary palp of the malaria vector mosquito *Anopheles gambiae*. Curr Biol. 2007; 17:1533–1544. [PubMed: 17764944]

Mayor C, Brudno M, Schwartz JR, Poliakov A, Rubin EM, Frazer KA, Pachter LS, Dubchak I. VISTA: visualizing global DNA sequence alignments of arbitrary length. Bioinformatics. 2000; 16:1046–1047. [PubMed: 11159318]

McIver SB. Sensilla of mosquitoes (Diptera: Culicidae). J Med Entomol. 1982; 19:489–535. [PubMed: 6128422]

McKenna MP, Hekmat-Scafe DS, Gaines P, Carlson JR. Putative *Drosophila* pheromone-binding proteins expressed in a subregion of the olfactory system. J Biol Chem. 1994; 269:16340–16347. [PubMed: 8206941]

Meijerink J, Braks MAH, van Loon JJA. Olfactory receptors on the antennae of the malaria mosquito *Anopheles gambiae* are sensitive to ammonia and other sweat-borne components. J Insect Physiol. 2001; 47:455–464. [PubMed: 11166310]

Mohanty S, Zubkova S, Gronenborg AM. The solution NMR structure of *Antheraea polyphemus* PBP provides a new insight into pheromone recognition by PBP. J Mol Biol. 2004; 337:443–451. [PubMed: 15003458]

Nei M, Gojobori T. Simple methods for estimating the numbers of synonymous and nonsynonymous nucleotide substitutions. Mol Biol Evol. 1986; 3:418–426. [PubMed: 3444411]

Nene V, Wortman JR, Lawson D, Haas B, Kodira C, Tu ZJ, Loftus B, et al. Genome sequence of *Aedes aegypti*, a major arbovirus vector. Science. 2007; 316:1718–1723. [PubMed: 17510324]

Rai KS, Black IV WC. Mosquito genomes: structure, organization, and evolution. Adv Genet. 1999; 41:1–33. [PubMed: 10494615]

Sandelin A, Wasserman WW, Lenhard B. ConSite: web-based prediction of regulatory elements using cross-species comparison. Nucleic Acids Res. 2004; 32:249–252.

Sandler BH, Nikonova L, Leal WS, Clardy J. Sexual attraction in the silkworm moth: structure of the pheromone-binding-protein-bombykol complex. Chem Biol. 2000; 7:143–151. [PubMed: 10662696]

Sengul MS, Tu Z. Characterization and expression of the odorant-binding protein 7 gene in *Anopheles stephensi* and comparative analysis among five mosquito species. Insect Mol Biol. 2008; 17:631–645. [PubMed: 18811600]

Sharakhova MV, Xia A, McAlister SI, Sharakhov IV. A standard cytogenetic photomap for the mosquito *Anopheles stephensi* (Diptera: Culicidae): application for physical mapping. J Med Entomol. 2006; 43:861–866. [PubMed: 17017220]

Syed Z, Leal WS. Maxillary palps are broad spectrum odorant detectors in *Culex quinquefasciatus*. Chem Senses. 2007; 32:727–738. [PubMed: 17569743]

Takken W, Knols BGJ. Odor-mediated behavior of afrotropical malaria mosquitoes. Annu Rev Entomol. 1999; 44:131–157. [PubMed: 9990718]

Takken W, van Loon JJA, Adam W. Inhibition of host-seeking response and olfactory responsiveness in *Anopheles gambiae* following blood feeding. J Insect Physiol. 2001; 47:303–310. [PubMed: 11119776]

Thompson JD, Gibson TJ, Pleawniak F, Jeanmougin F, Higgins DG. The ClustalX windows interface: flexible strategies for multiple sequence alignment aided by quality analysis tools. Nucleic Acids Res. 1997; 22:4673–4680. [PubMed: 7984417]

Vogt RG. Odorant binding proteins of the malaria mosquito *Anopheles gambiae*: possible orthologues of the OS-E and OS-F OBPs of *Drosophila melanogaster*. J Chem Ecology. 2002; 28:2371–2376.

Vogt RG, Riddiford LM. Pheromone binding and inactivation by moth antennae. Nature. 1981; 293:161–163. [PubMed: 18074618]

Vogt RG, Callahan FE, Rogers ME, Dickens JC. Odorant binding protein diversity and distribution among the insect orders, as indicated by LAP, an OBP-related protein of the true bug Lygus lineolaris (Hemiptera, Heteroptera). Chem Senses. 1999; 24:481–95. [PubMed: 10576256]

Vosshall LB, Amrein H, Morozov PS, Rzhetsky A, Axel R. A spatial map of olfactory receptor expression in the *Drosophila* antenna. Cell. 1999; 96:725–736. [PubMed: 10089887]

Wogulis M, Morgan T, Ishida Y, Leal WS, Wilson DK. The crystal structure of an odorant binding protein from *Anopheles gambiae*: Evidence for a common ligand release mechanism. Biochem Biophysics Res Commun. 2006; 339:157–164.

Xu PX, Zwiebel LJ, Smith DP. Identification of a distinct family of genes encoding atypical odorant-binding proteins in the malaria vector mosquito, *Anopheles gambiae*. Insect Mol Biol. 2003; 12:549–560. [PubMed: 14986916]

Xu PX, Atkinson R, Jones DN, Smith DP. *Drosophila* OBP LUSH is required for activity of pheromone-sensitive neurons. Neuron. 2005; 45:193–200. [PubMed: 15664171]

Zhou JJ, He XL, Pickett JA, Field LM. Identification of odorant-binding proteins of the yellow fever mosquito *Aedes aegypti*: genome annotation and comparative analyses. Insect Mol Biol. 2008; 17:147–163. [PubMed: 18353104]

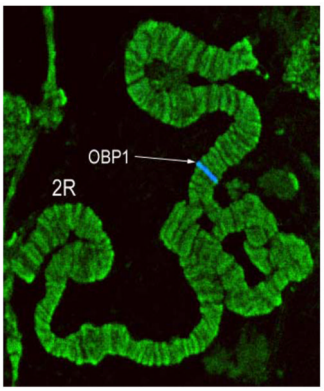

Figure 1.
Fluorescent in situ hybridization performed on the polytene chromosomes of *Anopheles stephensi*. The *An. stephensi* odorant-binding protein 1 gene (*AsteObp1*) is labelled with Cy5 (blue).

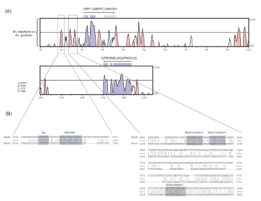

Figure 2.

Pairwise comparison between *Anopheles gambiae* and *An. stephensi* genomic sequences including the odorant-binding protein 1 (*Obp1*) gene and the nearby sequences. (A) VISTA plot that shows the alignment between *An. gambiae* and *An. stephensi*. The *x*-axis shows the relative position of the *An. gambiae* genomic DNA used as the reference genome in the alignment. The *y*-axis shows the % identity between the compared species. Arrows above the plots correspond to genes or coding sequences annotated in the *An. gambiae* genome according to the Ensembl database. The cut-off for sequence conservation is 75% over 100bp. The coding sequence portion of the third exon of the *Obp1* gene is only 18bp long, which is why it does not show a conserved peak. The boxed regions correspond to the conserved noncoding sequences that were further investigated for transcription factor binding sites. Coding regions are shown in purple, untranslated regions are in light blue, and conserved non-coding sequences are shown in pink. CNS, conserved noncoding sequences. UTR, untranslated region. (B) VISTA alignment between *An. gambiae* and *An. stephensi* corresponding up to 1 kb upstream of the *Obp1* transcription start site (boxed regions). Potential TFBS that are conserved for the two species are highlighted in the alignment. Three sites for two *Broad complex* isoforms are shown. The first and second *Broad complex-4* sites are reverse complementary.

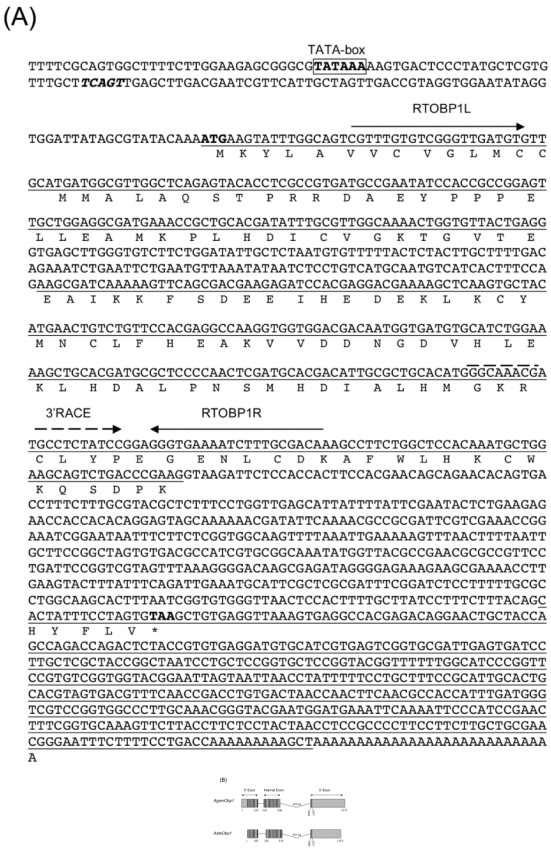

Figure 3.

Sequence and structure of anopheline odorant-binding protein 1 (*Obp1*) genes. (A) *Anopheles stephensi Obp1* genomic and cDNA sequences. The *AsteObp1* gene contains two introns among the three underlined exons. The deduced amino acid sequence of *Aste*OBP1 is shown below the coding regions. Start (ATG) and stop (TAA) codons are shown in bold. A putative initiator sequence, TCAGT, similar to the arthropod initiator consensus is in bold and italicized. The consensus for TATA-box, TATAAA, is shown in bold and boxed. The primers used in RT-PCR and RACE reactions are shown by arrows above the corresponding sequences. (B) *AsteObp1* gene structure is compared with that of *AgamObp1*. 5′ exons, internal exons, and 3′ exons are indicated. Boxes with vertical lines indicate open reading frames (ORFs) and they are connected with lines that indicate the introns. The 5′ and 3′ untranslated regions (UTRs) are shown in boxes with diagonal lines. Numbers indicate the relative positions of UTRs, ORFs and intronic regions.

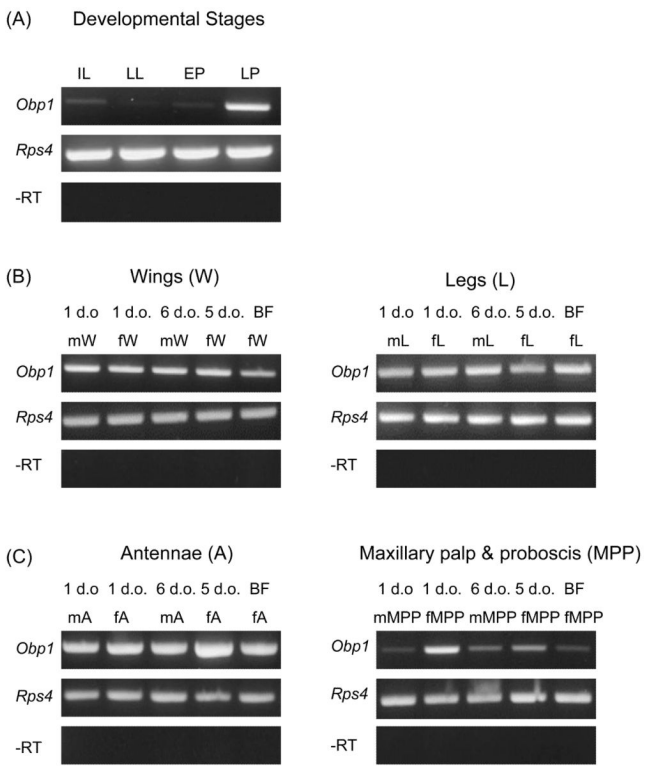

Figure 4.

Nonquantitative RT-PCR showing expression of *Anopheles stephensi* odorant-binding protein 1 gene (*AsteObp1*) in larvae and pupae (A), and chemosensory tissues of adult *An. stephensi* (B, C). Lanes are as follows: first instar larvae (IL), late larvae (LL), early pupae (EP), late pupae (LP); adult male wings (mW), adult female wings (fW), blood-fed female wings (BFfW); adult male legs (mL), adult female legs (fL), blood-fed female legs (BFfL); adult male antenna (mA), adult female antenna (fA), blood-fed female antenna (BFfA); adult male maxillary palp and proboscis (mMPP), adult female maxillary palp and proboscis (fMPP), blood-fed female maxillary palp and proboscis (BFfMPP). The *Rps4* internal control gene is used as the positive control. Minus reverse transcription (−RT) products (negative control without the use of reverse transcriptase) are also shown for each cDNA samples. d.o., days old. All RT-PCR reactions were performed with 35 cycles of amplification.

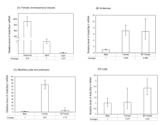

Figure 5.

Relative amount of the *Obp1* mRNA in adult chemosensory tissues of *An. stephensi*. The *y*-axis is the relative level of *AsteObp1* mRNA as determined by the $2^{-\Delta\Delta CT}$ method. Detailed data analyses are shown in Table 1 and Supplementary Material Tables S1-S3. The results are shown as the mean and a range specified by $2^{-(\Delta\Delta CT+SD)}$ and $2^{-(\Delta\Delta CT-SD)}$, where SD is the standard deviation, for three or more biological replicates each from independent collections. (A) Comparison of *AsteObp1* expression levels in different female chemosensory tissues. (B) Comparison of *AsteObp1* expression levels in the antenna of male, female and blood-fed females. (C) Comparison of *AsteObp1* expression levels in the maxillary palp and proboscis of male, female and blood-fed females. (D) Comparison of *AsteObp1* expression levels in the legs of male, female and blood-fed females. The relative amount of *AsteObp1* is significantly different between different chemosensory tissues in the females (Panel A; $P < 0.001$, One-way ANOVA with Tukey's post test). The relative amount of *AsteObp1* in antennae of non-blood fed females and blood-fed females, and the relative amount of *AsteObp1* in legs of male and female mosquitoes are not significantly different (Panels B-D) ($P > 0.05$, One-way ANOVA with Tukey's post test). In all cases, the calibrator sample for normalization show an average value of 1.

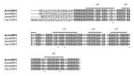

Figure 6.
Alignment of *Anopheles stephensi* odorant-binding protein 1 gene (*AsteObp1*) with its possible mosquito orthologues. All identical amino acid residues are shaded. The six conserved cysteines are shown in bold and indicated with asterisks. Predicted signal peptides are underlined in the sequences. The α-helices of *Aste*OBP1 are indicated by solid bars above the amino acid sequence. Species abbreviations are Aste, *Anopheles stephensi*; Agam, *Anopheles gambiae*; Aaeg, *Aedes aegypti*; Cqui, *Culex pipiens quinquefasciatus*.

Insect Mol Biol. Author manuscript; available in PMC 2011 February 1.

Table 1

Relative mRNA levels of *Anopheles stephensi* odorant-binding protein 1 gene (*AsteObp1)* in female antennae, maxillary palp and proboscis, and legs

Tissue		*Obp1*C_T	*Rps4*C_T	ΔC_T(*Obp1*C_T − *Rps4*C_T)	$\Delta\Delta C_T$(ΔC_T − ΔC_Tcalibrator)	Normalized *Obp1* amount relative to the calibrator, $2^{-\Delta\Delta CT}$
Antenna	replicate1	14.322	18.968	−4.647		
	replicate2	14.226	19.225	−5		
	replicate3	14.7	19.681	−4.982		
	Average	14.416 +/− 0.145	19.292 +/− 0.208	−4.876 +/− 0.254	−9.838 +/− 0.254	915 (767.5 − 1090)
Maxillary palp and Proboscis *	replicate1	23.73	18.08	5.651		
	replicate2	22.889	18.565	4.323		
	replicate3	23.183	18.272	4.912		
	Average	23.267 +/− 0.247	18.306 +/− 0.141	4.962 +/− 0.284	0 +/− 0.284	1 (0.82 − 1.217)
Legs	replicate1	28.209	18.913	9.295		
	replicate2	26.354	18.042	8.312		
	replicate3	27.125	18.35	8.776		
	Average	27.229 +/− 0.538	18.435 +/− 0.255	8.794 +/− 0.595	3.833 +/− 0.595	0.07 (0.046 − 0.106)

5-day-old female mosquitoes were used for each tissue collection.

Data presentation is according to Livak & Schmittgen (2001), with average and standard deviation (SD). Data in the final column are presented as the mean and a range specified by $2^{-(\Delta\Delta CT+SD)}$ and $2^{-(\Delta\Delta CT-SD)}$. All replicates are biological replicates.

* represents the calibrator.